WES-2025-283: Reply to Referee 1

Referee: "The authors proposed a general approach to account for flow curvature effects in Actuator Line (ALM) simulations of Vertical-Axis Wind Turbines (VAWTs). The new methodology was validated against wall-resolved simulations of a fictitious, single blade VAWT, proving its effectiveness in improving load predictions over one rotor revolution. The Reviewer believes that the topic is very interesting and worthy of investigation. The study is extensive and is supported by a solid theoretical framework."

Reply: we thank the referee for his positive global appreciation of our contribution to the simulation, using ALM, of flows with curvature effects such as those in vertical-axis turbines (VATs, for wind or water); also called cross-flow turbines. The study is indeed extensive and general, and the proposed methodology is shown to be very effective at predicting the time-evolution, over one blade revolution, of the loads (forces and moment). We put much effort in validating the proposed models against high-quality wall-resolved simulations of the fictitious single-blade VAT (previously studied by T. Villeneuve et al., by the U Laval group), and for different locations of the blade attachment point.

Referee: "Nonetheless, several aspects need improvement before publication:"

Reply: We answer below to the points by points comments/requests, and we modify the paper accordingly.

Referee: "1. Abstract: the abstract should be more concise and better highlight the impact and novelty of the work;"

Reply: We have shortened and improved the abstract. It is now:

"We revisit the modeling, using actuator line methods (ALM), of flow-curvature effects on airfoils and their application to vertical-axis turbines (VAT); which is important when the ratio of airfoil chord c to arm length R is not small. The models can only use the aerodynamic coefficients of the airfoil in uniform flow (here obtained using wall-resolved CFD of a NACA0015 airfoil at $Re_c = 6.0 \times 10^6$); they then consist in analytical modifications of those coefficients. The models for the normal force and moment coefficients use the classic analogy of potential flow with curved streamlines past an airfoil; their expression depends on the airfoil pitch angle and its attachment point to the arm. They are known, yet many authors have neglected the contribution of the aerodynamic moment. We here extend the models so as to cover all possibilities of attachment point and pitch angle, and up to near stall. Furthermore, we develop a new model for the tangential force (the analogy with that of potential flow being flawed): its inviscid part, that corresponds to negative drag, is required to compensate for the aerodynamic moment.

The improved models are first validated in steady flow corresponding the NACA0015 airfoil rotating with $\frac{c}{R} = \frac{2}{7}$. We cover the whole range of pitch angles, up to stall. The results are shown to compare well those of the reference CFD data. This validation is carried for two attachment points: at airfoil mid-chord and at quarter-chord.

An ALM incorporating the improved models is then also implemented in the CFD frame-

work, and is used to simulate the unsteady flow corresponding to a VAT configuration: the rotating NACA0015 airfoil without pitch placed in a free stream and operating at optimal tip speed ratio of of $TSR = 3.25$. This is also simulated for both attachment points. Here, a novel method is also developed to explicitly enforce the moment in an ALM. The various components of the ALM results are compared with those of the reference CFD data, and are found to be in good agreement throughout the rotation cycle."

Referee: "2. Introduction: flow curvature in VAWT is an old problem and there are many approaches available in the literature. The authors should better emphasize the novelty and advantage given by their method over the existing ones, such as the conformal mapping by Migliore (which is relatively similar to this one as an approach);

Flow curvature effects in VAWT is indeed an old problem. All approaches available in the literature use the analogy between a flow with curved streamlines around an airfoil without camber and a uniform flow past an airfoil with camber. This leads to the normal force coefficient $C_n(0)$ for a flat plate or thin airfoil without tilt angle recalled in Eq. (5); and which can then be associated to an effective shift in angle of attack by α_c recalled in Eq. (6): as would be the case for a cambered plate or thin airfoil. This is not new.

As stated in Akimoto et al (2013): "Migliore et al stated the virtual camber effect caused by the curved flow as shown in figure 1 (see their paper). However, these results do not show quantitative evaluation of the effect that is required to interpret the wind tunnel measurement of a two-dimensional (2D) wing to the condition of rotating VAWTblade." (Note that, in our case, "wind tunnel measurement" is to be replaced by "results of quality wall-resolved CFD simulations").

The subject of the paper by Akimoto et al (2013) is then to propose the conformal mapping that we recall in Eq. (3). The authors mention: "It provides bidirectional mapping between the two flow fields. For example, the flow around a symmetric wing in the curved flow is mapped to that around a curved (cambered) wing in the straight flow. Although the shape of mapped wing section is different from the original one, its aerodynamic coefficients show a good correlation to those of the original in the rotating condition. With the proposed method, we can reproduce the local f ow field around a rotating blade from the flow data around the mapped static wing in the straight flow condition."

We now recall better that contribution in the revised paper; and we also show that the statement of Akimoto et al is incorrect as far as the tangential force is concerned. We also develop a correct model for that.

Our paper is certainly not about developing a new conformal mapping, nor about reproducing the flow field around the airfoil, etc. It is about (1) developing corrections models for flows curvature effects for all three aerodynamic coefficients (normal force, tangential force, and moment); also showing that the potential flow analogy is flawed for the tangential force; and also proposing a correct model for it, (2) then confronting them to quality wall-resolved CFD data for steady flow of a rotating airfoil at various pitch angles, even up to both stall angles (that are different), also validating them to a good extent; (3) then implementing them

into an "ALM CFD setup" (by the way: itself also to be developed in the used CFD software) and confronting the ALM CFD obtained results to those of wall-resolved CFD data for the case of the unsteady flow of a rotating airfoil with a free stream (i.e., a VAWT configuration), and also validating them to a good extent; (4) finally, also developing a novel method for imposing an aerodynamic moment in an ALM method, and also validating it. All these elements are well contained in the abstract (now also improved) and in the introduction (that we also improve: see below).

In passing: please also note that we also propose a simplified version of the conformal mapping by Akimoto et al.: indeed, since $\frac{c/2}{R}$ is very small compared to unity in all cases of interest, the simple mapping that we propose in Eq. (5) largely suffices; and we indeed use it much in Section 3 (as detailed in our reply below to your next comment).

We have improved the introduction by adding, after the sentence "The effects of flow curvature were first studied by Migliore et al. (1980). In their work, they explore these effects using the concepts of "virtual camber" and "virtual incidence", the following:

"A bidirectional conformal mapping between the two flow fields was then also proposed by Akimoto et al. (2013) so that the flow around a symmetric airfoil in the curved flow is mapped to that around a cambered airfoil in the straight flow. They claim that the aerodynamic coefficients around the mapped airfoil show a good correlation with those of the original airfoil in the rotating condition and hence that they can approximately reproduce the local flow field around the rotating blade from the flow data around the mapped static wing in a straight flow. This is however incorrect as far as the tangential force is concerned: indeed, a straight potential flow past a cambered airfoil only has a normal force and an aerodynamic moment; whereas an inviscid flow past a rotating airfoil also has a tangential force. We will show that, and also propose a model for it."

Referee: "3. The theoretical framework is quite hard to follow. It is recommended to discuss the general theory (Sec. 3.5) first and then present the specific cases. This would also reduce the word count, which is quite substantial for this manuscript;"

We agree that it takes some effort to go through the theoretical framework; but we believe that this what is required to be complete, credible, and validated. We also stress that it follows a strong logic, with a step by step construction of the models, and accompanied by solid validation at required steps. More precisely:

1. First: We have the exact solution for the curved potential flow past a flat plate, presented in Appendix E (as it is quite involved mathematically). The streamlines for the plate at different tilt angles are presented in Section 3.1.

2. Second: The potential flow solution also suggests the "conformal transformation by Akimoto et al.": it is introduced in Section 3.2, and this is also where we present its "simplified form", which we use below for developing the models for forces and moments.

3. Third: The basis of the curvature correction for the normal force is that with the attachment point located at $x_p = c/2$, as in Appendix E. Hence this is why we first

cover this case, which constitutes Section 3.3.

(a) The basic case, also from Appendix E, Eq. (E25), is the normal force for the case without pitch angle: Section 3.3.1. We also recall the important aerodynamic moment $C_{m_{c/4}}$, as well as the notion of "angle of attack measured relative to the aerodynamic center" (which is the one used later in the ALM) and the correspoding C_l and C_d. All this is illustrated by Figure 2 (that uses the simplified form of the transformation).

(b) We then produce a model for the normal force for the case with pitch angle: Section 3.3.2. Our proposed model, Eq. (9) is not the classic model inspired from potential flow theory, Eq. (10). They are almost identical for small angles; yet they differ at large angles and we show later, in the validation for viscous flows, that our model is better at large angles, and even pretty good up to near stall angles.

There, we also produce a model for $C_{m_{c/2}}$ using potential flow theory past a cambered plate and we illustrate this in Figure 3 (that uses the simplified form of the transformation). We also produce the model for $C_{m_{c/4}}$. Finally, we also argue that the moment around the center of rotation of the arm must be zero in inviscid flow, and hence that there must be a tangential force to balance the moment $m_{c/2}$: Eq (14). This strong argument is also validated by an inviscid simulation (presented in Appendix D) and is most important as it forms the basis of our new model for the inviscid part of the tangential force, also valid for airfoils.

(c) In Section 3.3.3, we then present how the models are modified and enlarged (also for parasitic effects) when considering thin airfoils in real viscous flows.

(d) In Section 3.3.4, we finally confront our models to the reference data of wall-resolved CFD in Figure 4, and for the whole range of tilt angles, up to near stall. We think that this validates quite well our models, and that this constitutes a first essential step.

4. Fourth: The consider next the airfoil with its attachment point located at $x_p = c/4$, thus close to the aerodynamic center : this is Section 3.4. Here, we consider the flat plate and thin airfoils in one shot (to be concise), and we develop all models. This is also illustrated in Figure 5 for the case of the flat plate without pitch (and using again the simplified form of the transformation).

   This too requires a confrontation of the proposed models to the reference data of wall-resolved CFD, which is carried in Section 3.4.1 with Figure 6, also for the whole range of tilt angles, up to near stall.

5. Fifth: It is only when we have understood, and validated, how to model the case with $x_p = c/2$, and also the case with $x_p = c/4$, that we can generalize the modeling to all possibilites of x_p position. This generalisation is not trivial (it took some pain, trial and error). We strongly believe that presenting this Section first would mean presenting "equations inspired from God knows what" and would have no credibility.

Referee: "4. The numerical set-up of both ALM and wall-resolved simulations (timestep, numerical settings, near-wall treatment, etc...) is too limited for quality assessment and repeatability. Please provide more details;"

Reply: Please note first that the wall-resolved CFD simulations setup has also been validated against experimental data of pressure coefficient distribution along the airfoil chord at different spanwise location of a 3D wing (up to the near tip); this is also reported in Villeneuve et al. (2021). The reference simulations, and models, in the present paper being for 2D airfoils, we are very confident in the quality of our RANS results. We have added the following sentence at the begining of Appendix A:

"We note that the simulation setup has also been validated against experimental data of the pressure coefficient distribution along the airfoil chord, at different spanwise location of a 3D wing, and up to near the wing tip; this is reported in Villeneuve et al. (2021)."

To answer your request for more details, we have added the following in Section 6 on Results, just after the sentence "The tip speed ratio is $TSR = \frac{\Omega R}{U_w}$. The simulated case corresponds to $TSR = 3.25$, which is the value at which the produced power is maximized.":

"All simulations are conducted under the incompressible flow assumption. The ALM and wall-resolved simulations are performed using the finite-volume solver Siemens STAR-CCM+. The URANS equations are solved in conjunction with the Spalart-Allmaras turbulence closure model. A uniform velocity is imposed at the inlet, and a turbulent to molecular viscosity ratio of $\nu_t/\nu = 0.2$ is used, representative of a clean flow. A uniform static pressure is imposed at the outlet. The far lateral boundaries are symmetry planes.

Second-order schemes are employed for the spatial discretization of both the convective and diffusive fluxes. The temporal integration is carried using the second-order implicit unsteady scheme, and one turbine revolution is discretized into 1000 time steps. The pressure-velocity coupling is handled using the coupled flow algorithm for the ALM simulations to enhance numerical robustness, while the segregated approach SIMPLE is adopted for the wall-resolved simulations. The results reported correspond to simulations for which the relative variation of the cycle-averaged power coefficient is below 1%, thereby ensuring statistical convergence.

For the wall-resolved configurations, an overset mesh technique is used to accommodate the blade motion. To ensure adequate boundary layer resolutions, prismatic layers are used near the blade surface, with a target value of $y^+ \simeq 1$ for the height of the first cell, and a maximum wall-normal growth rate of 1.2. Two levels of mesh refinement are employed around the turbine: one for the turbine region, where the cell size is constrained by the overset mesh, and another one for the wake."

We have alslo modified slightly the description of the setup for the ALM at the beginnig of Section 6.1:

"The mesh used for the ALM simulations is shown in Figure 9. A rectangular domain is used, identical to that of the wall-resolved reference case. An overset technique is implemented to maintain a hexahedral mesh with the same template for the ALM ($h = \sigma/2$) as used in Sections 4 and 5. The overset approach also enables the rotation of the actuation zone. Two refinement regions are used: one for the turbine region, including the template, and another one for the wake. The cell size within the turbine region is chosen so as to ensure accurate interpolation between that region and the background mesh. Notably, the wall-resolved reference case mesh is more refined ($\simeq$ 328,000 cells) compared to the ALM mesh ($\simeq$ 37,000 cells),

in line with the intended efficiency of the ALM approach. The methodology is applied to all ALM cases in this work."

We have also improved the caption of the figure:

"Computational domain and mesh used for the ALM simulations. The turbine region, including the template of the ALM, is implemented using an overset mesh approach to enable the 2-D template as described in Sections 4 and 5. The weights for the application of the forces are also illustrated in blue."

Referee: "5. Section 4: given the problem at hand and the use of a more detailed smearing function as the one proposed for the pitching moment, a kernel of c/4 seems quite coarse. Was a sensitivity analysis performed?"

No sensitivity analysis was performed on the ratio σ/c for the template used for imposing the moment (as explained in Section 5); nor is it needed.

Indeed, we already wrote in the paper: "We extend the actuator line method to enable the distribution of an aerodynamic moment. Of course, a pure aerodynamic moment cannot be imposed, as the ALM uses a distribution kernel of some size σ. We hence replace the aerodynamic moment by a force field that has the same net effect, as presented in Figure 7; and we then discretize this force field using the 2D template."

Thus, by construction, our method imposes the net moment whatever the choice of σ. We hence used the same value of $\sigma = c/4$ as that used for imposing the forces (as described in Section 4); also for simplicity. We have added such a statement at the end of Section 5:

"We stress that our method imposes the net moment whatever the choice of σ. We hence can use the same value of σ as that used for imposing the forces, also for simplicity."

As mentioned in the paper, this choice corresponds to the recommendation by Martinez et al. who tuned an ALM for a symetric airfoil in uniform flow (thus only imposing the forces as the aerodynamic moment is zero). We also wish to stress that the choice of $\sigma = c/4$ is not "coarse": In a recent paper, they even revisited their recommendation, and they now propose to use $\sigma = 2\,c/5$: see J. Fluid Mech. (2025), vol. 1024, A15, doi:10.1017/jfm.2025.10870.

Now: the important parameter is the discretization of the kernels: the ratio of grid size h to mollification parameter σ. Obviously, the smaller h/σ, the finer the numerical discretization of those kernels. We have collected much experience in ALM when testing the Gaussian kernel for imposing the forces: we have tried $h/\sigma = 1/3$, $2/5$ and $1/2$: the lift and drag results are essentially identical. We have also verified that one should not use $h/\sigma > 2/3$, as the Gaussian is then no longer properly discretized. The choice $h/\sigma = 1/2$ is finally retained as it is the cheaper in terms of resolution. Note also that, because we integrate exacty the kernel over each cell of the template (see Eqs. (52) and (53), and Table 1), we ensure that the net forces are completely imposed to the flow solver. We have added such a statement in Section 4:

"As the kernel was integrated over each cell of the template, we ensure that the forces are completely imposed to the flow solver."

Concerning the ratio h/σ used for discretizing the kernel used for imposing the moment: using the same ratio $h/\sigma = 1/2$ leads to the weights of Figure 8 and Table 2. Again, because we integrated the kernel components over each cell of the template (see Eqs. (63) and (64), and Table 2), we also ensure that the net moment is completey imposed to the flow solver. This is indeed the case when we examine the results obtained on the ALM of a VAT configuration (Sections 6.1.2 and 6.1.3, with Figures 10 to 12). We have added also such a statement at the end of Section 5:

"As the two components of the kernel were integrated over each cell of the template, we ensure that the moment is completely imposed to the flow solver.

Referee: "6. Was an unsteady aerodynamics model used in the ALM simulations? Given the high c/R radius and so average reduced frequency, it is expected to have a notable impact on the results;"

Reply: No unsteady aerodynamic model was used for the ALM simulations; nor is it needed. Indeed, the $TSR = 3.5$ value is high enough that the flow past the blade does not separate dynamically at any position on the cycle; as is seen when examining the vorticity field of the wall-resolved simulations. Hence, using the static flow polar data (lift, drag and moment coefficients) of the NACA0015 airfoil, solely corrected for flow curvature effects, shoukd here be sufficient to obtain ALM simulation results that are accurate; as is indeed confirmed later by the obtained results. Please also note that, when an ALM is used for an unsteady flow, vorticity is continuously shed into the wake, as it should; hence, the Biot-Savart velocity induced by this wake vorticity is properly taken into account when we measure the effective velocity (see Section 4).

In fact, it is because we know, from previous wall-resolved simulations of the present single-blade fictitious VAT by T. Villeneuve, who performed simulations that span the full range of TSR values, that $TSR = 3.5$ corresponds to the case of maximum power production AND without significant boundary layer separation. We have added the following at the beginning of Section 6.1:

"This value is also high enough that the flow past the blade does not separate dynamically at any position over the cycle; as is confirmed when examining the vorticity field of the wall-resolved simulation in Figure 13. Hence, using the static airfoil polar data, solely corrected for flow curvature effects (i.e. no added dynamic polar model), is expected to be sufficient."

Side note: For significantly lower TSR values, say $TSR = 2.5$, the span of angles of attack seen by the blade over the cycle becomes larger, and it would become necessary to also include unsteady corrections to model the dynamic effects on the polar (even possibly dynamic stall effects); for instance using the Leishman and Beddoes dynamic airfoil polar model. For instance, P. Rochefort did a study with a stagiaire (M. Mordret) of a VAT configuration with $R/c = 6$ operating at $TSR = 2.5$: some results are shown in Figure 1. It is seen that a dynamic model for the airfoil polar is required in addition to the corrections for flow curvature

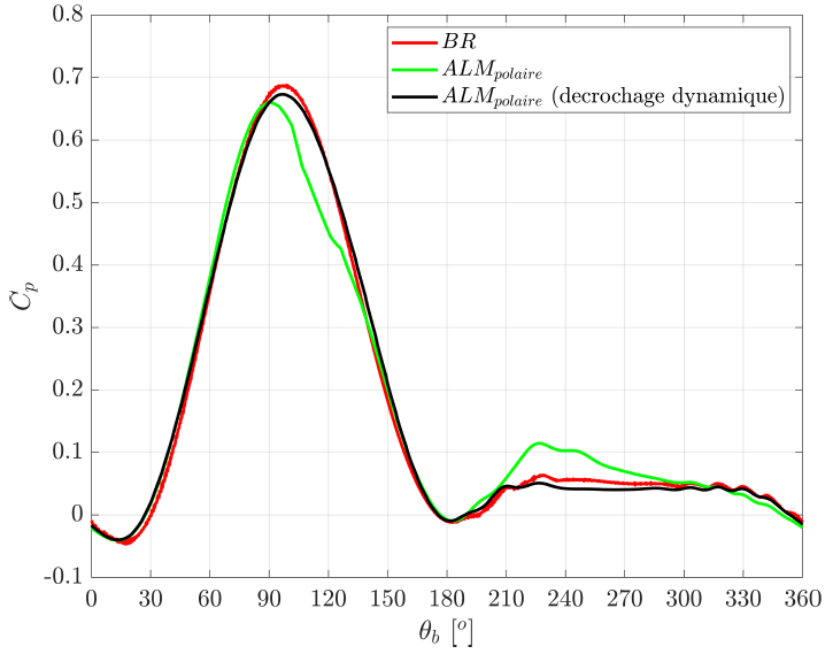

Figure 1: Illustrative results of ALM simulations for the case of a VAT configuration with $R/c = 6$ operating at $TSR = 2.5$; courtesy of P. Rochefort and M. Mordret. Power coefficient for the reference wall-resolved CFD (red), for the ALM using the static airfoil polar model and the corrections for flow curvature effects (green), ALM using a dynamic model for the aifoil polar and the corrections for flow curvature effects (black).

effects; and it is also seen that combining both produces results that compare quite well with those of the reference wall-resolved CFD.

Referee: "7. Section 6: It would be more effective to add the case without correction, to quantify the impact of the proposed method;"

Reply: It is well knwon that an ALM without corrections for flow curvature effects produces very poor results, in all cases. To show that effectively, as you request, we have added this case in Figures 10 and 11, and in Table 3. The results are indeed very poor.

Referee: "8. Section 6: The authors discussed that their method is valid for relatively thin airfoils. It would be interesting to test it on one of the thicker ones actually used in VAWT design, such as the NACA0018 or 0021."

Reply: Recall that the present correction for flow curvature effects has multiple components. The correction for the normal force is obtained from the analogy with the curved potential flow solution past a flat plate with pitch; also presented in Appendix D. There, Eq. (E25) provides the normal force coefficient when the pitch is zero. The factor $\left(\frac{c}{2R}\right)^2$ in the denominator is always very small compared to 1 (it is here equal to $\left(\frac{1}{7}\right)^2 = \frac{1}{49} \simeq 0.020$). Hence, as is discussed in the paper, the factor is neglected and we simply use $C_n(0) = -2\pi \frac{c}{4R}$ as correction for flow curvature effects on a flat late or thin airfoil. (Note that we could have kept it, but it would just have made the correction model more complicated, for very little added value.)

This being: we think that it would be interesting, and useful, to further improve the correction model for the normal force by ALSO taking into account the airfoil thickness, in addition to taking into account the flow curvature. We offer, in confidence, that this would "simply" require to revisit Appendix D and consider there an airfoil with chosen thickness instead of a flat plate. This can most certainly be done for Joukowsky-type airfoils; but we leave it to the (near) future.

Now, and given that we only used the theoretical correction on the normal force obtained for a flat plate airfoil, we elected to test it on the NACA0015: because it is also the airfoil studied previously by Villeneuve et al. at U. Laval in his PhD thesis and in various papers (also that of 2021 with G. Winckelmans as co-author), and for which they had produced the aerodynamic data. We stress that the NACA0015 is not "very thin", and hence it already stresses/challenges a little bit the correction model.

Given that the ALM results obtained using the present correction for the normal force are indeed very good for the NACA0015, it is likely that they will still be quite good for the NACA0018; and maybe still acceptable for the NACA0021. (Again: we would prefer to first improve fthe correction model for the normal force by ALSO taking into account theoretically the airfoil thickness.)

Last but not least: for any airfoil considered: we need to (1) produce the detailed aerody-

namic data in uniform flow and as a function of the angle of attack using wall-resolved CFD (see Appendix A), then perform blade resolved CFD in VAT configuration so as to obtain reference data, then perform the ALM simulation to compare to the reference: this amount to a lot of work! And the paper is already quite long.